

Experimental Study of Snap-Fits Using Additive Manufacturing

Kevin Torossian¹ and David Bourell²

¹National Engineering School of Saint-Etienne, 42023 Loire, France

²Laboratory for Freeform Fabrication, Mechanical Engineering Department, The University of Texas at Austin, TX 78712

Abstract

A snap-fit is a mechanical joint system whose mating parts exert a cam action, flexing until one part slips past a raised lip on the other part, preventing their separation. The use of snaps in additive manufacturing (AM) is an approach for assembling components of parts too large to build in one piece in AM. There are broadly two types of snap-fits possible to encounter, permanent and non-permanent, depending on the design geometry. An experimental study was carried out to evaluate the mating/dismounting force for snap-fits regarding several geometrical parameters for additive manufacturing. The design chosen for this study has been established from the start to work on only one design. The parameters chosen for experimental investigation were the mating angle, the separation angle and the inner diameter of the mating part. All in all, fifteen pairs were designed and additive manufactured for evaluation. The force required to insert and separate the snap components was recorded and compared to the value based on a derived equation.

Introduction

Snap-fits are a simple, quick and cost effective method of assembling two parts. When designed properly, parts with snap-fits can be assembled and disassembled numerous times without any effect on the assembly. Depending on the application, snap-fits can also create a permanent assembly. Snap-fits are also an environmentally friendly form of assembly because of their ease of disassembly, making components of different materials easy to recycle. Elimination of adhesives is also an environmental advantage. Although snap-fits can be designed with many materials, the ideal material is thermoplastic because of its high flexibility. Other advantages include its relatively high elongation, low coefficient of friction, and sufficient strength and rigidity to meet the requirements of most applications.

There has always been a desire to build parts that are larger than the AM fabrication build chamber. Typically components are glued and/or dove tailed together after building. The purpose of this experimental study was to verify if snap-fits fabricated with AM could be used to attach components to one another, for plastic parts at least. Applications exist where the assembly would be permanent, or in some cases, it could be desirable to take the assembly apart. That is why the required force for snapping and unsnapping is important.

The development of equations for the detailed sizing of snap-fit features and for predicting their response can be accomplished using analytical, numerical or experimental methods. As shown in Figures 1 and 2, several types of design for snap-fits exist including different cross sectional shape and thus diverse equations to calculate the mating/dismounting force [1].

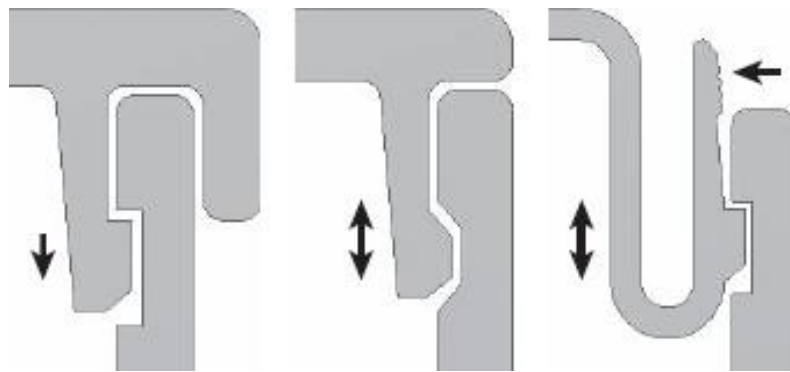


Figure 1: Different examples of snap-fits design [1]

Type of design	Shape of the cross section	A	B	C	D
1 Cross section constant Over the length	Rectangle	$y = 0.67 \cdot \frac{\varepsilon \cdot l^2}{h}$	$y = \frac{a + b_{(1)}}{2a + b} \cdot \frac{\varepsilon \cdot l^2}{h}$	$y = K_{(2)} \frac{\varepsilon \cdot l^2}{r_2}$	$y = \frac{1}{3} \cdot \frac{\varepsilon \cdot l^2}{c_{(2)}}$
2 All dimensions in direction y, e.g., h or α , decrease to One-half		$y = 1.09 \cdot \frac{\varepsilon \cdot l^2}{h}$	$y = 1.64 \cdot \frac{a + b_{(1)}}{2a + b} \cdot \frac{\varepsilon \cdot l^2}{h}$	$y = 1.64 \cdot K_{(2)} \cdot \frac{\varepsilon \cdot l^2}{r_2}$	$y = 0.55 \cdot \frac{\varepsilon \cdot l^2}{c_2}$
3 All dimensions in direction z, e.g., b and a, decrease to one-quarter		$y = 0.86 \cdot \frac{\varepsilon \cdot l^2}{h}$	$y = 1.28 \frac{a + b_{(1)}}{2a + b} \cdot \frac{\varepsilon \cdot l^2}{h}$	$y = 1.28 \cdot K_{(2)} \cdot \frac{\varepsilon \cdot l^2}{r_2}$	$y = 0.43 \cdot \frac{\varepsilon \cdot l^2}{c_{(2)}}$
Deflection force	1,2,3	$P = \frac{bh^3}{6} \cdot \frac{E_i \varepsilon}{l}$	$P = \frac{h^2}{12} \cdot \frac{a^2 + 4ab_{(1)} + b^2}{2a + b} \cdot \frac{E_i \varepsilon}{l}$	$P = Z_{(4)} \cdot \frac{E_i \varepsilon}{l}$	$P = Z_{(4)} \cdot \frac{E_i \varepsilon}{l}$

Figure 2: Equations regarding snap cross sectional shape and design [2]

Figure 3 illustrate the snap-fit design chosen for this experimental study. The cross section is a circular cross section constant over the length.

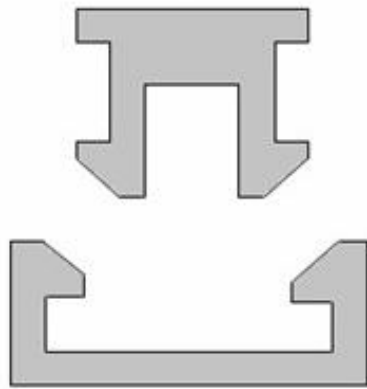


Figure 3: Chosen design [3]

Due to cost and time issues, the experimental method is usually replaced by a numerical method using the finite element method to simulate experiments. In this case, analytical and experimental results have been compared. In the following several sections, the analytical and experimental formulations will be discussed in detail.

Derived Equation

As shown in Figure 2, the equations for the permissible deflection and the deflection force are given, which toadied in deriving an equation for the mating/dismounting force [1].

$$F_m = P * \left| \frac{\mu + \tan \alpha}{1 - \mu * \tan \alpha} \right| * n$$

$$F_m = \frac{b(D_1 - D_0)^2}{24} * \frac{E\epsilon}{L} * \left| \frac{\mu + \tan \alpha}{1 - \mu * \tan \alpha} \right| * n$$

$$\begin{cases} P = \frac{bh^2}{6} * \frac{E\epsilon}{L} \\ h = \frac{D_1 - D_0}{2} \end{cases}$$

$$\text{But, } \delta = \frac{PL^3}{C_1 EI} = \frac{PL^3}{3E \frac{bh^3}{12}}$$

With $C_1 = 3$, regarding the load on a rectangle cross section.

$$\sigma = \frac{Mc}{I} = \frac{PL^2}{\frac{bh^3}{12}} = \frac{6PL}{bh^2} = E\epsilon \quad \Longleftrightarrow \quad E = \frac{6PL}{bh^2\epsilon}$$

$$\text{So, } \delta = \frac{12PL^3bh^2\epsilon}{18PLbh^3} = \frac{2L^2\epsilon}{3h} \iff \epsilon = \frac{3h\delta}{2L^2}$$

$$F_m = \frac{b(D_1 - D_0)^2}{24} * \frac{3E\left(\frac{D_1 - D_0}{2}\right)\delta}{2L^3} * \left| \frac{\mu + \tan \alpha}{1 - \mu * \tan \alpha} \right| * n$$

$$F_m = \frac{b(D_1 - D_0)^2}{8} * \frac{E\delta}{L^3} * \frac{(D_1 - D_0)}{4} * \left| \frac{\mu + \tan \alpha}{1 - \mu * \tan \alpha} \right| * n$$

$$F_m = \frac{b(D_1 - D_0)^3}{32} * \frac{E\delta}{L^3} * \left| \frac{\mu + \tan \alpha}{1 - \mu * \tan \alpha} \right| * n$$

The nomenclature is included at the end of this article. With this derived equation, the mating/dismounting force can be analytically calculated by altering geometrical parameters and thus positively impacting the snap-fit design. According to prior research [1], the equation to have the dismounting force, F_d , is the same as the one above but with α being replaced by α' .

Moreover, the derived equation takes into account not only the geometrical parameters but also the mechanical properties of the material such as the Young's modulus and the friction coefficient.

Experimental

As mentioned earlier, only one design has been chosen, and, to see the most representative evolution of the force, some geometrical parameters have been set. On the other hand, the inner diameter D_0 , the mating angle α and the separation angle α' were varied during the study. The material used for this study was polyamide 12 (nylon), so the mechanical properties such as E and μ were also set during the whole study.

The only parameter which was assigned arbitrarily was the permissible deflection δ ; it has been set to be 1 mm. This parameter indeed depends on the permissible strain in outer fibers ϵ which value was not known. A finite element simulation would have been necessary to obtain the value of ϵ .

Once all the parameters had been fixed, fifteen snap-fit pairs including fifteen top parts and bottom parts were designed. An example of a pair is shown in Figures 4 and 5.

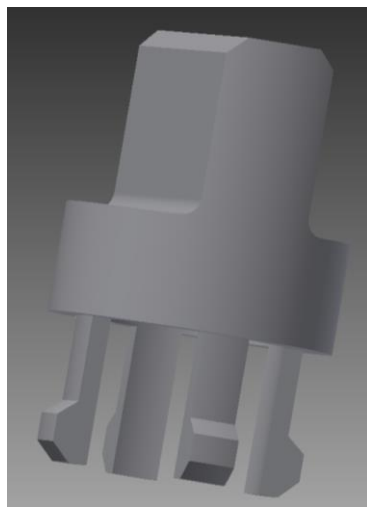


Figure 4: Top part

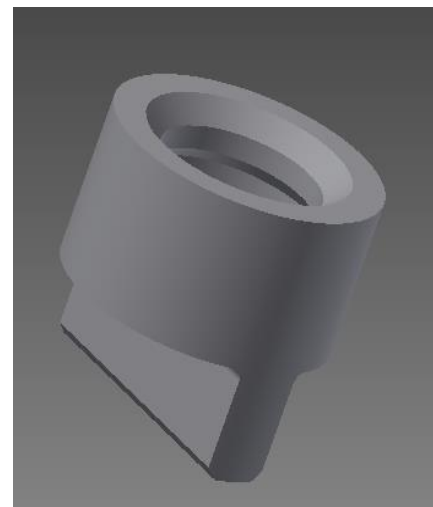


Figure 5: Bottom part

Figure 6 shows the three geometrical parameters that have been varied for this study.

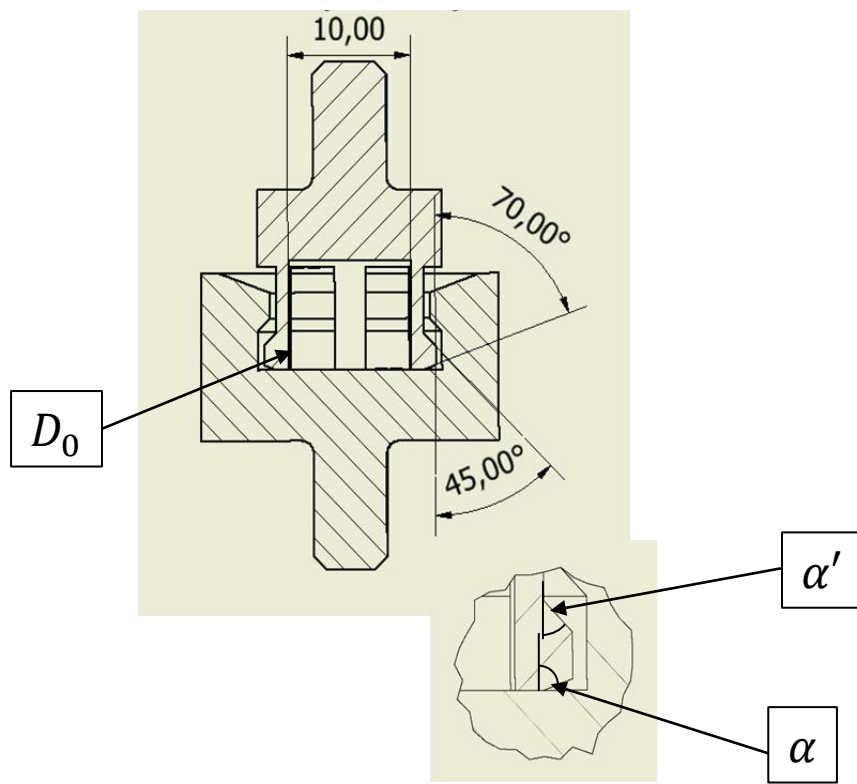


Figure 6: Detailed drawing of a pair

A 3D Systems HiQ Sinterstation with StablTemp capability was used to fabricate the samples. In this study, six different separating angles have been tested (30° , 40° , 50° , 60° , 70° , 90°), as well as, five different mating angles (30° , 40° , 50° , 60° , 70°) and four different inner diameters (4 mm, 6 mm, 8 mm, 10 mm).

The loading tests made on the pairs of samples were tension and compression tests, performed using a 500 N capacity Instron universal tester. The results were recorded and compared to the values obtained with the derived equation. Clamps were used during the tests to achieve best possible colinearity between the top part and the bottom part.



Figure 7: Tension test of a pair

Results and Discussions

According to Figures 8 and 9, the values found with the derived equation seem to be close to the results found experimentally, although the experimental curves do not exactly follow the ones plotted with the analytical results. This can be explained because of the difficulty to get a perfect collinearity between the two parts during the tests. Moreover, obtaining an identical contact at the same moment for the four branches is extremely complicated when the force is applied on the snap-fits which resulted in some non-representative results.

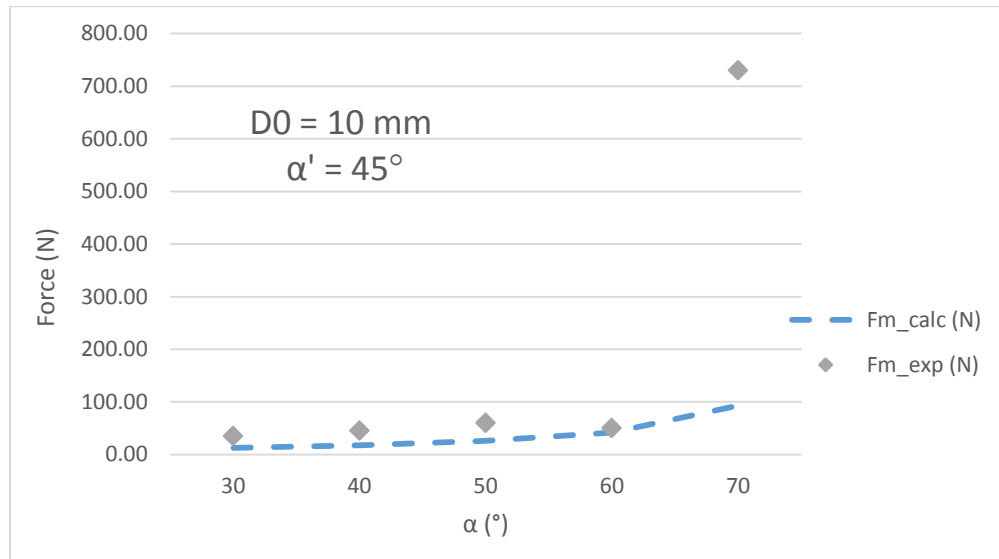


Figure 8: Mating force as a function of the mating angle

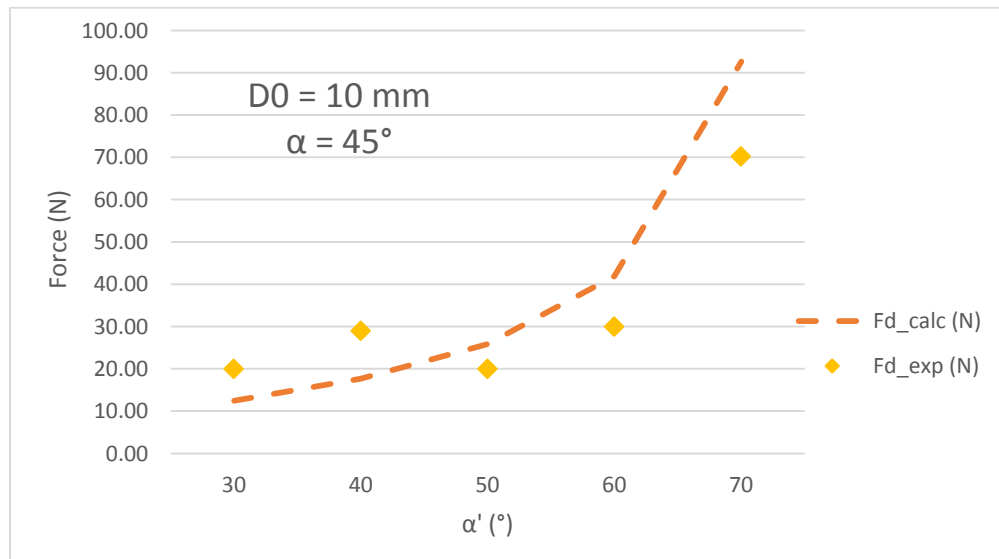


Figure 9: Dismounting force as a function of the separation angle

The gap present for $\alpha = 70^\circ$ is especially large, because the sample broke during the compression test. This can perhaps be avoided with a larger contact surface between the two parts.

Figure 10 shows a sizeable difference when comparing the analytical and experimental results. This is most likely due to the same issue as mentioned for the two graphs above.

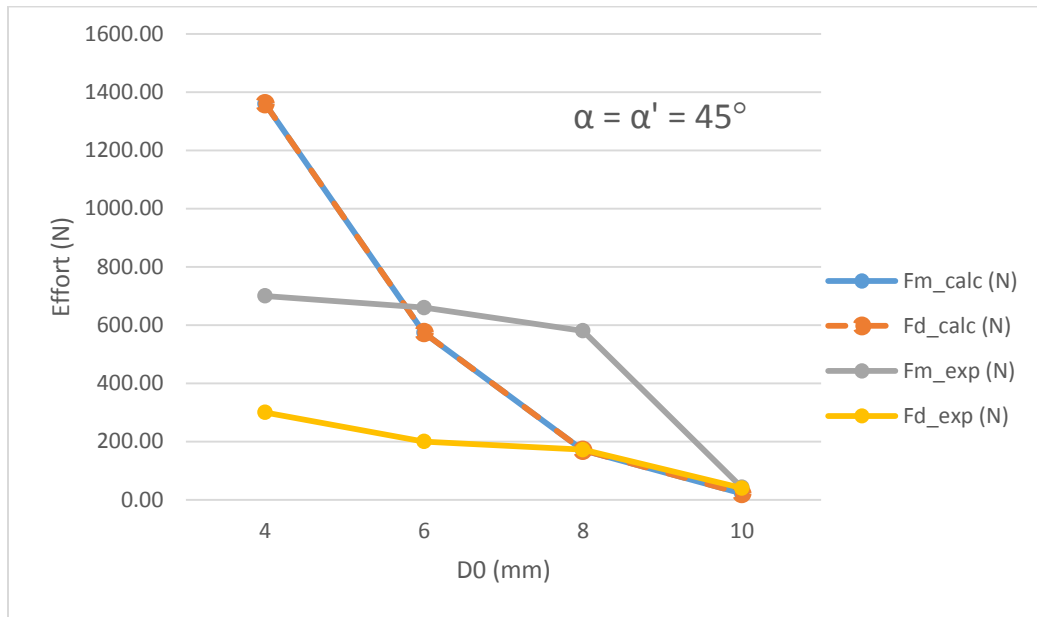


Figure 10: Mating / Dismounting force as a function of the inner diameter

Overall, the force values obtained for tension tests and compression tests where $\alpha = \alpha'$ are not the same. Indeed, the force value should be the same whether it is in tension or in compression, according to the derived equation.

A possible explanation of this observation is the presence of some degree of buckling during the compression tests when the load is applied on the top part to mate with the bottom part. This results in the bowing of the top part's four branches during this phase and thus more load is necessary to counter this effect.

However, this model has its limits. In fact, when α or α' reach 80° , (value that has been found by interpolation between 70 degrees and 90 degrees), instead of having higher force values, lower values have been obtained with the derived equation. The reason why the force decreases comes from this part of the derived equation : $\frac{\mu + \tan \alpha}{1 - \mu * \tan \alpha}$. In this case, both the numerator and the denominator tend quickly to infinity which creates an indeterminate form. Thus, $\lim_{\alpha \rightarrow 90} \frac{\mu + \tan \alpha}{1 - \mu * \tan \alpha} \sim -\frac{1}{\mu}$, it follows that the obtained coefficient is inferior to the previous ones starting from $\alpha = 80^\circ$.

Conclusions

An experimental study has been done on polyamide 12 snap-fits, fabricated with a Selective Laser Sintering machine, by performing compression and tension tests on fifteen paired samples. The results obtained were compared to analytical results obtained using a derived equation. The geometrical parameters chosen to make the comparison were the mating angle α , the separating angle α' and the inner diameter D_0 . After analyzing the results, work must be done on the current model to take into account the buckling effect during the compression/mating and to allow to understand more fully why the equation seemingly breaks down for higher angle values.

Despite this fact, this model seems to be accurate for angles between 30° and 70° . However, perfect collinearity and identical contact for the four top part branches are required during the tests to obtain representative results. All in all, additive manufactured snap-fits can be integrated in systems during CAD to print them directly on the main part. This provides a means to attach components to one another, for plastic parts at least.

Acknowledgments

One of the authors (KT) performed this work while on an undergraduate internship at the University of Texas at Austin. He acknowledges the internship program at his home institution, National Engineering School of Saint-Etienne.

Nomenclature

F_m : mating force

F_d : dismounting force

P : deflection force

D_1 : outer diameter

D_0 : inner diameter

μ : friction coefficient

E : Young's modulus

α : mating angle

α' : separating angle

σ : permissible stress

ϵ : permissible strain in outer fiber

b : width of arm

h : thickness of arm

δ : permissible deflection

L : length of arm

M : force moment

c : distance between outer fiber and neutral fiber

n : number of arms

References

- [1] <https://www.safaribooksonline.com/library/view/mastering-autodesk-inventor/9781118016824/ch019-sec009.html>
- [2] Snap-Fit Joints for Plastics - A Design Guide – Bayer MaterialScience
http://fab.cba.mit.edu/classes/S62.12/people/vernelle.noel/Plastic_Snap_fit_design.pdf
- [3] https://es.wikipedia.org/wiki/Snap_fit
- [4] Technical Expertise - Snap-Fit Design Manual - BASF
<http://web.mit.edu/2.75/resources/random/Snap-Fit%20Design%20Manual.pdf>
- [5] Selection and Optimization of Snap-Fit Features via Web-Based Software - Tieming Ruan, Ph.D. Dissertation, 2005, Ohio State University, Mechanical Engineering